Coordinating Demand Response Aggregation with LV Network Operational Constraints

Valentin Rigoni, Student Member, IEEE, Damian Flynn, Senior Member, IEEE, and Andrew Keane, Senior Member, IEEE.

***Abstract*-- High shares of renewable energy resources are increasing the value of using demand response (DR) mechanisms to enhance the resiliency and efficiency of power system operation. In this context, residential DR is expected to become an increasingly important asset. In order to exploit this resource, DR aggregators are expected to combine the capabilities of a large group of householders and participate, as a single provider, in the electricity market. In doing so, it is imperative for aggregators to consider the operational constraints of the local network. Otherwise, the quality of the electricity service can be jeopardized and the true DR potential overestimated. This paper presents a novel methodology that integrates DR aggregators with distribution network operators for a secure and efficient scheduling and real-time operation of DR in residential radial feeders. The method is evaluated on a real unbalanced feeder where DR provision (from a mix of technologies) is coordinated with the network steady-state thermal and voltage limits. In this study, with the corresponding data seasonality and controllable devices, it is shown that complying with network operational constraints can impose, at certain times, a significant limit to the allocation of DR.**

***Index Terms*—Demand aggregator, demand response, distributed energy resources, optimization, system flexibility.**

I. Main Nomenclature

Variables:

P_{total_t}, Q_{total_t}	Total active/reactive DR power consumption
$P_{h,t}, Q_{h,t}$	House aggregated active/reactive DR power consumption
$Y_{i,t}$	Key network electrical variable
P_t^{SETS}	SETS total active power consumption
$P_{t,s}^{SETS,ch}, P_{t,s}^{SETS,bst}, P_{t,s}^{SETS,dis}$	SETS charge, boost and discharge power
$E_{t,s}^{SETS}$	Energy stored in SETS device
P_t^{ESS}	Total ESS active power consumption
$P_t^{ESS,ch}, P_t^{ESS,dis}$	ESS charge and discharge active power
SOC_t^{ESS}, SOC_t^{EV}	ESS and EV state of charge
P_t^{EV}	EV charge active power
P_t^{EWH}	EWH active power consumption

Parameters:

H	Number of customers participating in DR
$t_{init}^{schedule}$	First time step of DR scheduling
$t_{init}^{operation}$	Current DR operation time step
$\sigma_{P_t}, \sigma_{Q_t}$	System signal for the provision of active and reactive power from DR
$\alpha_{P_t}, \alpha_{Q_t}$	Penalization on operational deviations for the active and reactive power from DR
$P_{total_t}^*, Q_{total_t}^*$	Scheduled DR network active/reactive power
$Y_{forecast_{i,t}}^*$	Forecasted value of the component of Y_i due to non-controllable demand
$c_t^{Y_i,P_h}, c_t^{Y_i,Q_h}$	Active and reactive power sensitivity coefficients for variable Y_i
N	Number of time steps per hour
η_s^{SETS}	Hourly efficiency of SETS device
$E^{SETS,init}$	Stored energy of SETS for first time step
$\eta^{ESS,ch}, \eta^{ESS,dis}$	ESS charging and discharging efficiency
$SOC^{ESS,init}$	State of charge of ESS for first time step
η^{EV}	EV charging efficiency
$SOC^{EV,start}$	State of charge of EV when arriving home
$SOC^{EV,init}$	State of charge of EV for first time step
T_{EV}^a	Time step at which EV arrives home
T_{EV}^f	Time step when EV should be fully charged
$T_{morning}^{pk}, T_{evening}^{pk}$	Hot water demand peak time steps
$E_{morning}, E_{evening}$	Hot water demand peak required energy
$E_{morning}^{init}, E_{evening}^{init}$	Hot water demand peak consumed energy prior to first time step

where:
$SETS$: smart electric thermal storage
ESS: energy storage system
EV: electric vehicle
EWH: and electric water heater

This work was supported by Science Foundation Ireland under the SFI Strategic Partnership Programme Grant Number SFI/15/SPP/E3125.

II. Introduction

THE power system is facing significant changes, motivated by considerable growth in the share of renewable energy sources (RES), such as solar and wind generation. With RES providing a substantial contribution to generation capacity, system operators are interested in increasing system flexibility. Flexibility can help cope with unforeseen changes in generation, reduce market electricity price volatility, maximize the output from RES and improve the overall reliability and efficiency of the power system [1], [2]. This background has raised the opportunity and benefits that demand response (DR) can have in system operation [1].

Understood as a modification to the normal consumption pattern of end-use customers, residential DR has gained recent traction due to the increasing adoption of distributed generation, and technologies for the electrification of the transport and heating sectors [3], [4]. As the expectation is for many of these technologies to be widely adopted by householders, their DR capabilities could be very valuable if suitably exploited. Previous work has shown that, with adequate incentives,

residential DR can increase the penetration of RES, result in lower electricity prices and reduce customers' electricity bills while meeting their energy needs [5]–[9]. However, the fact that customers are integrated through a distribution grid is commonly disregarded. In low voltage (LV) distribution systems with significant aggregation of customers and impedance paths (e.g. in Europe), the local network will impose limitations, at certain times, to DR mechanisms that cannot be neglected if assessing, at scale, their true contribution [10].

A number of publications have tackled the coordination of DR with network operational constraints [11]–[15]. The authors in [11] formulate an optimal power flow (OPF) problem, where aggregators and customers, through an interactive process, agree on an optimal DR schedule. In [12], modeling of building thermal operation is incorporated into a 3-phase unbalanced OPF problem for the provision of DR from electric storage space heaters. A method for frequency and voltage regulation from thermostatically controlled loads (TCLs), using a centralized OPF formulation, is proposed in [13]. The authors in [14] introduce linearized AC power flow equations, for balanced medium voltage (MV) systems, in an OPF problem that adjusts the power at the head of the feeder using the capabilities of the local distributed energy resources (DER). In [15], a balanced chance-constrained OPF problem, that accounts for RES uncertainties, is proposed. This method assumes DR to be obtained from aggregations of TCLs located at the MV buses. While these studies successfully highlight the importance of grid limitations, no distinction between LV grid operation (where residential customers are located) and DR operation is considered. It is expected, however, for these tasks to be performed by different agents. Firstly, residential DR is likely to be operated by aggregators that combine the capabilities of residential customers and participate, on their behalf, in the electricity market [16], [17]. Secondly, it is the distribution network operator (DNO) that will have to ensure, with often limited available monitoring infrastructure, that the electricity service is not jeopardized. Note that not only may DNOs not have an interest in providing DR services, but they may be prevented from doing so by regulatory agencies [18]. Consequently, a framework that integrates aggregators and DNOs will become imperative.

Two possible frameworks for aggregator/DNO coordination have been recently discussed in [19]. In the first, aggregators receive a constraint on load action (e.g. maximum power for a group of loads). In the second, DNOs can block aggregator decisions over certain loads, based on the network state. However, there is no discussion on how it is expected that DNOs will take their corresponding decisions. Without an appropriate method, DNOs may only be able to ensure safe network operation by being overly conservative. In addition, the proposed formulations do not consider a future time horizon, which impedes efficient operation of day-ahead DR schedules and does not guarantee compliance with customer requirements (e.g. electric vehicles should be fully charged by a certain time). This paper presents a novel methodology for practical coordination of residential DR with LV network operational constraints. Under the proposed framework, representative data exchange between DNOs and DR aggregators enables the latter to formulate a series of equations, of low computational complexity, that effectively serve to construct the constraints associated with the local network operational limits. The method is tested for the scheduling and real-time operation of DR in a real LV feeder, where aggregators are incentivized to allocate power consumption, from multiple electrical devices, based on a time of use electricity price. Key contributions can be summarized as:

- A framework that identifies DNOs and aggregators as separate agents and enables the latter, via a limited exchange of representative information, to coordinate DR within the local LV network operational constraints
- A set of independent linear and quadratic equations, obtained by aggregators using the data received by the DNO, that characterize the magnitude of the network variables as a function of the DR allocation

III. Methodology

It is not expected for aggregators to be responsible for network modeling, monitoring and operation (leaving these tasks to the grid operator). However, incorporating constraints that account for network limits into DR day-ahead scheduling and real-time operational problems can ensure that the electricity service is not jeopardized, and that true DR capability is utilized. This section describes how, using representative data provided by the DNO, aggregators can formulate a set of novel equations, (9)-(10), that effectively characterize the magnitude of those network variables that are considered as key for safe network operation by the DNO (e.g. critical node voltages) as a function of the DR allocation.

In the above context, a novel framework (summarized in Fig. 1) identifies four participants of the DR scheme, namely: DNOs, aggregators, customer energy management systems (EMSs) and the power system (i.e. the market for DR services). Note that here, a group of aggregators operating in the same local network will be treated as a single entity, as the mechanics behind their coordination are out of scope for this work. This section begins by introducing the concepts of DR day-ahead scheduling and real-time operation using generic formulations. Then, it describes the state estimation and sensitivity analysis techniques used by the DNO to generate representative data that is provided to aggregators (i.e. estimations of the magnitude of the network variables and their sensitivities to the power consumption from those customers providing DR). Finally, it shows how aggregators can obtain the proposed equations (9)-(10), used to formulate the network operational constraints.

A. Aggregators' DR Scheduling and Real-Time Operation

In general, the potential benefits for all the participants in the DR mechanism can be related to a system signal, varying in time, that incentivizes the DR allocation [7], [20]. Here, aggregators will maximize the allocation of DR at the most beneficial times based on two signals: $\boldsymbol{\sigma}_P$ and $\boldsymbol{\sigma}_Q$, representing suitably accurate predictions of the system needs for active and reactive power respectively (e.g. for active power: predicted day-ahead electricity prices).

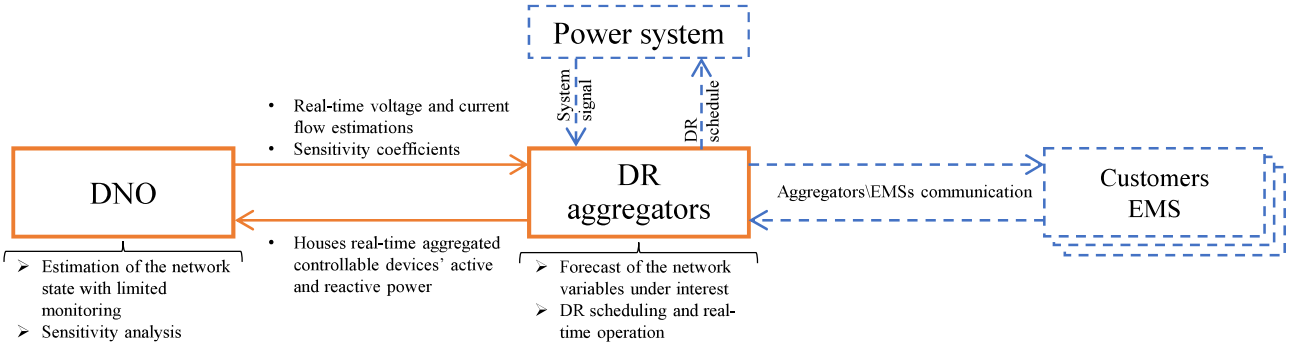

Fig. 1. Proposed framework for DR implementation. All novel features incorporated by this method are highlighted with solid lines, focusing on aggregators/DNO coordination, and the resulting decisions communicated to other participants

1) Demand Response Schedule

A DR schedule can be obtained by solving the constrained multi-period optimization (1)-(4), where P_{total_t} and Q_{total_t} are the scheduled sum of all active and reactive power consumptions from the controllable devices in the network. Note that the objective function is written in its minimization form, where σ_{P_t} and σ_{Q_t} are weights for each time step t of the scheduling time horizon T. The optimal values for P_{total_t} and Q_{total_t} must comply with constraints (2)-(4). Constraint (2) represents the network operational constraints, where $Y_{i,t}$ are the variables, k in total, considered as key by the DNO for safe operation; e.g. the voltage magnitude at those customer point of connection (CPOC) with the highest impedance path to the head of the feeder (i.e. expected to experience large voltage variations) or the current flows at the main cable branches. These variables are confined to be within their statutory limits, Y_{min_i} and Y_{max_i}. Additionally, the set of equalities $g_j(\boldsymbol{x}) = y_j$ and inequalities $f_u(\boldsymbol{x}) \geq d_u$ represent the operational constraints of the controllable devices and the customer requirements; e.g. ensuring that operation of electric space heaters does not result in room temperatures outside a comfort range. The parameters defining (2)-(4), during time-period T, are forecasted by the aggregators.

$$\min \sum_{t_{init}^{schedule}}^{T} \left(\sigma_{P_t} P_{total_t} + \sigma_{Q_t} Q_{total_t}\right) \quad (1)$$

subject to:

$$Y_{min_i} \leq Y_{i,t} \leq Y_{max_i} \;\; with \; i = 1, \dots, k \quad (2)$$

$$g_j(\boldsymbol{x}) = y_j \;\; with \; j = 1, \dots, q \quad (3)$$

$$f_u(\boldsymbol{x}) \geq d_u \;\; with \; u = 1, \dots, w \quad (4)$$

where

$P_{total_t} = \sum_h^H P_{h,t}$, $Q_{total_t} = \sum_h^H Q_{h,t}$

Once (1)-(4) are solved, aggregators obtain the optimal DR schedule across the future time horizon T. Crucially, this schedule not only accounts for the type and characteristics of the controllable devices and the customer requirements but also for the network steady-state operational limits, through (2).

2) Real-time Demand Response Operation

It is possible for the DR schedule to be infeasible, during operation, due to differences between the forecasted parameters in (2)-(4) and the real-time state of the network and operational characteristics of the controllable devices. Consequently, the DR dispatch may need to be adjusted based on up-to-date information (available to aggregators at every control step of the following day). Based on the above, at each control step ($t_{init}^{operation}$) during real-time operation, aggregators solve an optimization problem with the objective (5); the last two terms represent penalties for discrepancies with the original schedule.

$$\min \sum_{t_{init}^{operation}}^{T} \left(\begin{matrix} \sigma_{P_t} P_{total_t} + \sigma_{Q_t} Q_{total_t} \\ + \alpha_{P_t} \left\| P_{total_t} - P^*_{total_t} \right\| + \alpha_{Q_t} \left\| Q_{total_t} - Q^*_{total_t} \right\| \end{matrix} \right) \quad (5)$$

The real-time operational problem is defined by (5) subject to (2)-(4). Constraints (2)-(4) are updated at each control step, with their forecasted parameters (for the remaining steps in T) changing based on new information (e.g. new network variables). The proposed problem adapts the DR dispatch to real-time conditions while complying with the schedule.

B. Obtaining the Network Operational Constraints in (2)

Aggregators are not expected to have access to network data and monitoring equipment; however, they can rely on data, provided by the DNO, to formulate the constraints in (2). This subsection will describe: 1) information that DNOs must provide to aggregators, and how to obtain it, and 2) how aggregators can combine this information to produce a set of equations characterizing the network variables in (2) as a function of the DR allocation.

1) Representative Data Produced by the DNO

Provided that the DNO has access to adequate measurements and a sufficiently accurate network model, it can provide aggregators with: a) an estimation of the network variables $Y_{i,t}$ and b) sensitivity coefficients describing the changes for each $Y_{i,t}$ due to changes in the power consumed by those customers enrolled in the DR scheme.

a) Estimations of the Network Variables $Y_{i,t}$

For the purposes of this paper, it is proposed that the DNO estimates the magnitude of the network variables by means of least squares estimation (LSE), the most common formulation in state estimation [21]. Assuming a Gaussian distribution for the error of all M measurements, LSE consist of minimizing the likelihood formula in Equation (6), where $E(z_m)$ and σ_m are the expected value and standard deviation of the m^{th} measurement, z_m, respectively. For most state variables, $E(z_m)$ is expressed as a power flow equation relating them to z_m.

$$\min \sum_{m}^{M} ([z_m - E(z_m)]/\sigma_m)^2 \quad (6)$$

While it is expected that monitoring capabilities will increase at LV distribution feeders with the implementation of smart grid technologies [6], widespread network monitoring is not expected to be available for near-term implementation of active network management strategies [22]. Therefore, in order to achieve observability, it is expected that pseudo-measurements will be used to compensate for the partial lack of real measurements [23]. The LSE used in this work adopts the approach in [23], and replaces all power consumptions from the non-controllable loads with statistical pseudo-measurements. As a result, at every control step, the DNO solves the problem in (6), with a vector of z_m measurements composed of:

- actual measurements of the 3-phase voltages and active/reactive power flows at the head of the feeder.
- actual measurements of the active and reactive power consumptions at each CPOC from the DR devices (communicated to the DNO by the aggregators).
- pseudo-measurements for the expected value and the standard deviation of the active and reactive power consumptions from the non-controllable demand of the customers in the feeder.

Note that the equations used to relate every measurement z_m with the state variables (i.e. $E(z_m)$) are those of the conventional three-phase power flow problem using the current injection method from [24]. However, if required, improved formulations could facilitate scalability and robustness [25]. In addition, pseudo-measurements can be eventually replaced by actual measurements if the monitoring infrastructure is improved (e.g. with smart meters).

b) Network sensitivity coefficients

Given that aggregators have no access to network data, DR allocation cannot result from the solution of a conventional OPF problem [19]. However, network sensitivity coefficients, proven to provide accurate results under multiple topologies and DER [26]–[29], can be used to quantify the variation in the network variables, $Y_{i,t}$ in (2), due to changes in the power consumed by each customer enrolled in the DR scheme.

While there exists multiple sensitivity analysis methodologies, the method used in this work is based on that proposed in [28], proven to be effective for LV unbalanced feeders. However, as the DNO has access to the most likely state of the system from the LSE solution, there is no need to explore multiple offline scenarios, as in [28]. Consequently, the sensitivity analysis from [28] is simplified and limited to: first, allocating, at each node, the power injections obtained from the LSE solution; then, solving a series of AC power flows under different values of the active or reactive power at each CPOC (at the time), by modifying the latter in regular intervals within an upper and lower bound. The results from these power flow calculations are used in a linear regression [30] that characterizes the variables under interest with a linear model:

$$Y_{i,t} = a_{i,t} + c_t^{Y_i,P_h}\Delta P_h \quad (7)$$

$$Y_{i,t} = a_{i,t} + c_t^{Y_i,Q_h}\Delta Q_h \quad (8)$$

where the slope of the linear functions (7)-(8), $c_t^{Y_i,P_h}$ and $c_t^{Y_i,Q_h}$, are the sensitivities of variable Y_i to the active and reactive power consumptions at house h, respectively (i.e. quantifying how much the network variable $Y_{i,t}$ will change due to ΔP_h and ΔQ_h). The overall process is exemplified in Fig. 2 for the generic case of a remote CPOC voltage vs phase b active power variations at a local CPOC; as customers are single-phase, sensitivities will differ from phase to phase.

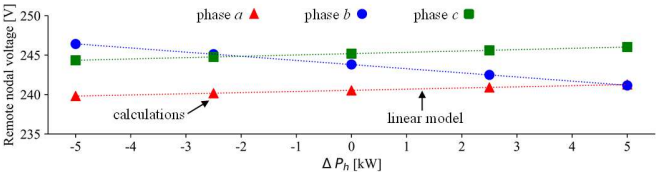

Fig. 2. Remote nodal voltage vs. active power consumptions at a phase b CPOC.

The order of the regression model proposed in [28] (and in regression analysis in general) is empirical and results from analysis of the training data [30]. An over-fitted model would unnecessarily increase the computational difficulty of the problem (higher degree for Equations (9)-(10)) and could result in ill-conditioned regressions [30].

2) Set of Equations Characterizing the Magnitude of the Network Variables Y_i as a Function of the DR

Using the network variable estimations and sensitivity coefficients obtained from the DNO, aggregators can express the magnitude of the variables $Y_{i,t}$ in (2) with the novel equations (9), for nodal voltages and active and reactive power flows, and (10), for current and complex power flows:

$$Y_{i,t} = Y^*_{forecast_{i,t}} + \sum_h^H c_t^{Y_i,P_h} P_{h,t} + \sum_h^H c_t^{Y_i,Q_h} Q_{h,t} \quad (9)$$

$$Y_{i,t}{}^2 = \left[\Re\left(Y^*_{forecast_{i,t}}\right) + \sum_h^H c_t^{\Re(Y_i),P_h} P_{h,t} + \sum_h^H c_t^{\Re(Y_i),Q_h} Q_{h,t}\right]^2 + \left[\Im\left(Y^*_{forecast_{i,t}}\right) + \sum_h^H c_t^{\Im(Y_i),P_h} P_{h,t} + \sum_h^H c_t^{\Im(Y_i),Q_h} Q_{h,t}\right]^2 \quad (10)$$

Both the DR scheduling and subsequent operation are multi-period problems that account for future time-horizons. The latter must be reflected in the constraints and expressions in (2)-(4). For network constraints, the value of $Y_{i,t}$ in (9)-(10) is decomposed into two components: one from non-controllable demand, $Y^*_{forecast_{i,t}}$, and another one due to DR (i.e. additional terms using the sensitivity coefficients). The value of $Y^*_{forecast_{i,t}}$ (i.e. forecasted state of the network under the sole presence of non-controllable demand at each time step) can be obtained by aggregators with the following procedure:

1) Create a data set with the values of $Y_{i,t}$ estimated by the DNO over previous periods of time which are similar to the future time horizon T (e.g. if T is a typical weekday, use estimations from previous similar weekdays).
2) The impact, over every $Y_{i,t}$, of past known DR actions is removed from the obtained data set using the sensitivity coefficients, as in equation (11) for the case of voltages, and active and reactive power flows. The result is a new data set comprised of the component of each variable $Y_{i,t}$ relating only to the non-controllable demand: $Y^*_{i,t}$.
3) The new data set feeds a forecasting method that provides the values of $Y^*_{i,t}$ during T: $Y^*_{forecast_{i,t}}$.

$$Y^*_{i,t} = Y_{i,t} - \sum_h^H c_t^{Y_i,P_h} P_{h,t} - \sum_h^H c_t^{Y_i,Q_h} Q_{h,t} \quad \forall t \in T^* \quad (11)$$

In (10), the decomposition of $Y_{i,t}$ into its real and imaginary parts recognizes changes in the direction of flow. For instance, in a network with batteries, current flows will decrease (compared to the case with no batteries) if their injected power is less than the local demand. However, from the point that the batteries injected power exceeds the local demand, current flows will instead increase [31]. Such phenomena cannot be captured by a single sensitivity coefficient, such as (9).

The novel equations in (9)-(10) express the network variables (for each time step of the DR time horizon) as a function of the DR allocation. Therefore, (9)-(10) enable aggregators to formulate the set of network constraints in (2), where each network variable $Y_{i,t}$ is constrained within its statutory limits. Compared to conventional power flow equations, aggregators do not need access to the network admittance matrix and are therefore not responsible for network modeling; this task, together with estimation of the network state are the responsibility of the DNO. Crucially, this distinction between the roles of operators and aggregators is a key contribution to near-term deployment of residential DR mechanisms. In addition, the linear and quadratic expressions in (9)-(10) present low computational complexity, facilitating scalability of scheduling and real-time operational problems. Note that these expressions are independent (e.g. voltage at node i is not expressed as a function of any other state variable) and only those network variables that need to be regulated must be incorporated into the optimization problem. The accuracy of (9)-(10) will be validated in Section V.

IV. Test System

The methodology is tested on a real representative LV feeder where DR is allocated based on a time-of-use electricity price. While there is a potential market for reactive power from residential DR (provision of reactive power is an ancillary service for voltage regulation [32]), reactive power consumption from controllable devices is neglected in this test case, given that the near-term implementation of DR mechanisms is focused on enhancing system capacity and providing ancillary services for frequency stability [6], [32].

A. System Signal Model

A system signal is required to justify the DR service. For this study, two day-ahead electricity price signals are obtained from the Irish Single Energy Market Operator [33]. Therefore, the objective in (1) will adjust the timing of operation of customers' controllable resources, in order to take advantage of lower price periods and, consequently, minimize electricity payments. Both signals are depicted in Fig. 3, together with the forecasted wind generation profiles [34], and correspond to two generic weekdays. Signal 1 presents a situation where evening prices decrease due to a wind generation peak. On the other hand, Signal 2 shows a more common situation where prices are higher during system morning and evening demand peaks [35], due to the commitment of expensive peak generation. Note that evening prices for Signal 2 are greater than those for Signal 1 despite having a higher wind generation contribution; this is due to circumstantial commitment of more expensive generation. In

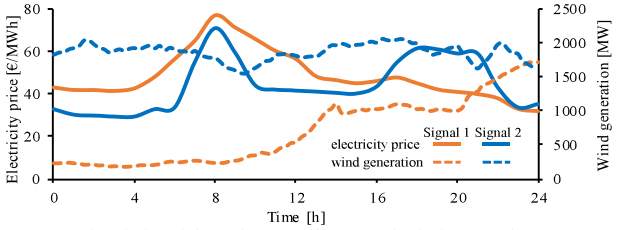

Fig. 3. Day-ahead electricity prices and forecasted wind generation [33]-[34]

terms of network impacts, Signal 1 will tend to promote an evening allocation of DR that coincides with the peak demand, i.e. overloading further the network assets. In contrast, Signal 2 promotes DR allocation at times of lower loading. Price signals are assumed to be independent of the DR schedule. In reality, the day-ahead market would incorporate the capacity offered by DR [36], affecting electricity prices. However, accounting for the latter would not affect the mechanics behind the proposed DR coordination with network operational limits.

B. Controllable Electrical Devices

The methodology presented in Section III is independent of the type of controllable electrical devices. In order to emphasize this point, a mix of technologies is considered: smart electric thermal storage (SETS), energy storage systems (ESS), electric vehicles (EV) and electric water heaters (EWH), each of them presenting different characteristics. For example, EVs and EWHs generally require that a certain volume of energy is consumed before a given time of day, with EVs not always connected to the network. In the case of ESS, energy drained from the grid can be stored and later dispatched when convenient. SETS can store electricity in the form of heat, enabling heating demand to be shifted while maintaining comfortable room temperatures.

The mathematical models of the considered devices are briefly presented in Appendix A. The expressions describing their operational characteristics are included in (3)-(4). It is assumed that aggregators have full knowledge of the characteristics of these devices and can perform direct control actions, through the EMSs. This assumption is taken for simplicity and transparency, and to place an upper bound on load response. However, during actual operation, the downside of such centralized approach would likely be large computational times. Nonetheless, note that the validity of expressions (9) and (10), and therefore of the proposed DR coordination with network constraints, will be independent of the manner that aggregators interact with EMSs.

C. Non-Controllable Demand

The daily demand profiles, allocated to each house, for the non-controllable demand are obtained using the residential load model from [35], which generates residential demand profiles with varying load composition (accounting for occupancy, appliances, etc.). Note that electric space heaters and water heaters are removed from [35] as these devices, providing DR services, will be modeled separately.

Expected values and standard deviations of the non-controllable demand pseudo-measurements in the LSE algorithm, from Section III.B.1, are obtained from an aggregated sample of the above-mentioned profiles.

D. Network Model

The analysis is implemented on a real LV feeder from a set of UK networks [37] (network 12, feeder 2). This feeder shows the same topology as that of the most common representative feeder which will show voltage and thermal problems due to the presence of DER [38]. The study feeder supplies power to 83 single-phase customers and is illustrated in Fig. 4. It is assumed that 12.5, 15, 25 and 50% of the houses in the feeder have ESS, EVs, SETS, EWHs, respectively; all these technologies are randomly allocated and used in the DR scheme. The above-installed capacities are chosen to achieve similar loading effects on the obtained DR dispatches.

The presence of the upstream MV network will be seen as a varying voltage at the head of the LV feeder, affecting the operating voltages of all nodes. Therefore, a varying voltage profile, see Fig. 5, is assumed at the head of the feeder so that the calculation of the network sensitivities used in equations (9)-(10) is perform under realistic circumstances.

The size of the optimization problems from Section III will be proportional to the number of customers in the feeder. In that regard, a feeder of 83 customers is in line with what is expected to be encountered in European-style systems. For instance, the results from [38] show that 98.7% of British LV feeders have less than ~100 customers. The Australian representative feeders obtained in [39] have an average and maximum number of customers of 47 and 105, respectively. In addition, typical Dutch LV feeders present less than 70 customers [40].

V. Results

The efficiency of the methodology at coordinating the DR schedule and operation with the feeder's voltage and thermal limits, according to the system signals in Fig. 3, is tested. Fig. 6 gives a representation of the scheduling and real-time operation processes. Simulations are performed for a typical weekday with a 10-minute control step. The forecast for $Y_{i,t}^{*}$, $Y_{forecast}^{*}{}_{i,t}$ is obtained with a 30-minute resolution, based on the LSE results from the previous 4 weekdays, using the SARIMA method from Python's Statsmodels library [41], which supports the direct modeling of the seasonal component of the training data. The obtained forecasts are interpolated to coincide with the 10-minute resolution of T. For the network constraints, six key network variables (shown to be critical for RES integration [28], [42]) are identified: the 3-phase voltages at the node with the highest impedance path to the head of the feeder and the 3-phase current flow at the main cable section. Even if performing day-ahead DR scheduling, the time set T is composed of a 36 h time horizon. Limiting T to only 24 h neglects some of the constraints associated with the operation of controllable devices, i.e. the time at which customers require their EVs to be fully charged extends beyond the first 24 h. Finally, it is assumed that aggregators can extend the profiles in Fig. 3 for the additional 12 h period using forecasting techniques.

Network sensitivities are calculated at each control step. First, the power injection/consumption at every node is defined based on the results from the LSE. Then, from the perspective of each CPOC, local active power consumption is varied in 25% intervals in the range -5 to +5 kW. At each step, a power flow

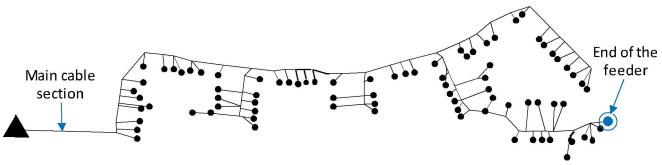

Fig. 4. Test feeder: dots are houses while the triangle is the head of the feeder

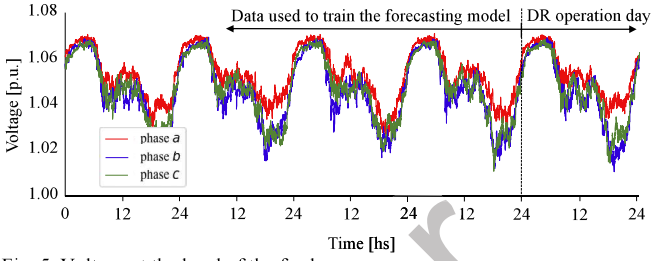

Fig. 5. Voltage at the head of the feeder

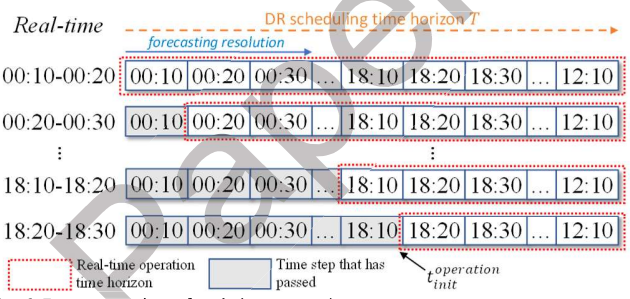

Fig. 6. Representation of real-time operation process

simulation is solved using OpenDSS [43] and the magnitude of all variables $Y_{i,t}$ is stored. This compilation of values is used to train the models in (7) and (8). Regression analysis theory states that, for good predictive performance, the data samples need to properly describe the trend of the related variables. Therefore, the number and granularity of intervals must be adequately defined based on training data observations [27]. Here, intervals of 25% were found to be adequate. It needs to be considered that unnecessarily small intervals will lead to higher computational times.

In this test, the scheduling and operational problems, together with the DNO's LSE, are programmed in Pyomo [44] and solved using Knitro [45]. Particularly, the first two problems, defined by (1)-(4) and by (5),(2)-(4), are quadratically constrained non-convex optimization problems due to the expressions, in the form of (10), used for the main cable current flows. The non-convexity of the problems implies that global optimality of (1) and (5) is not guaranteed; this means that it is possible that the solver will converge to a local optimum and, thus, result in a sub-optimal use of the DR resources. It is important to note that while equations in the form of (10) are not convex, no convexity issues were encountered during any of the simulations performed in Section V. Feasible solutions may be prioritized in front of approaching a globally optimal solution to ensure safe network operation and compliance with customer constraints. In this context, if convexity was seen as a requirement, a possible solution would be to impose limits on the active and reactive power flows, with the linear expressions (9), as proposed in [19]. The counterpart is that the limits in (2) may have to be more conservative. Finally, note that the models used for the controllable devices

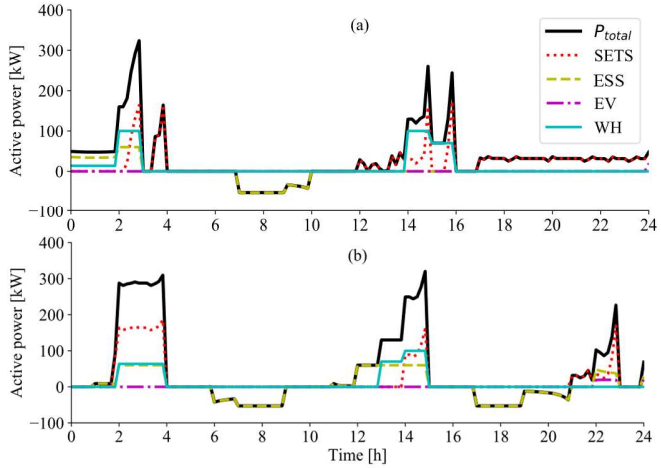

Fig. 7. DR schedule: Signal 1 (a) and Signal 2 (b) neglecting network constraints

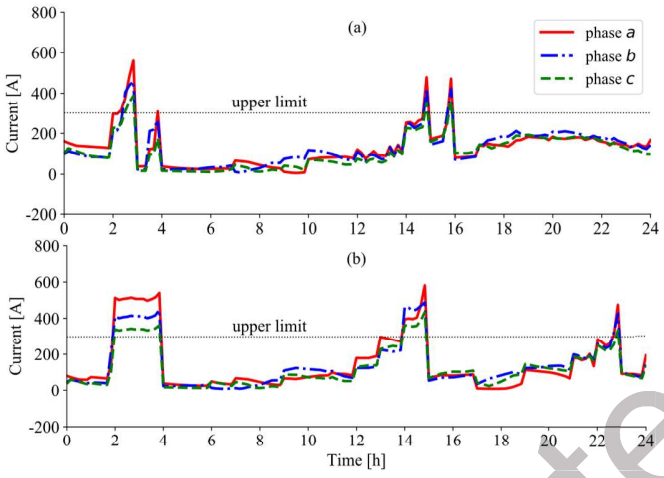

Fig. 8. Expected current at the main cable section for the DR schedule for Signal 1 (a) and Signal 2 (b) neglecting network constraints

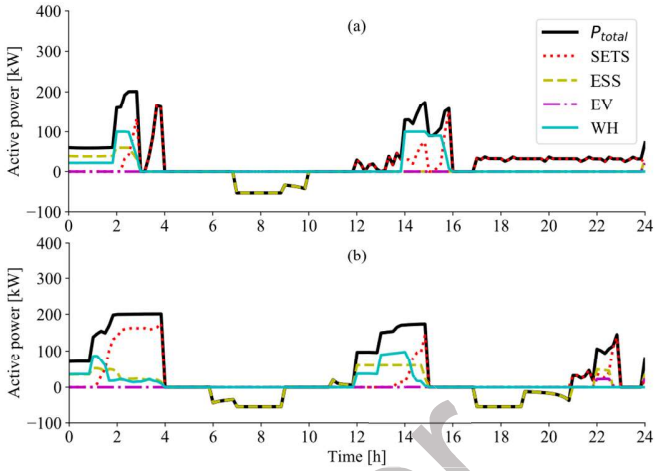

Fig. 9. DR schedule: Signal 1 (a) and Signal 2 (b), with network constraints

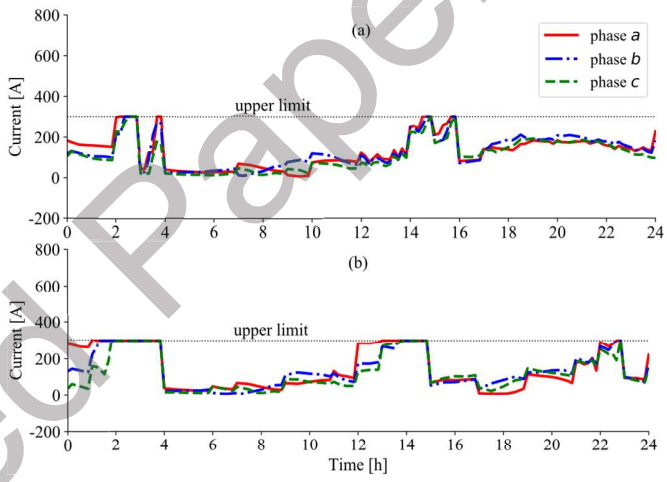

Fig. 10. Expected current at the main cable section for the DR schedule for Signal 1 (a) and Signal 2 (b), with network constraints

can always incorporate more complex non-linear equations and integer variables, resulting in different types of optimization programming.

A. Scheduling of the Demand Response

In order to highlight the importance of coordinating DR mechanisms with network constraints, a DR schedule is obtained for each of the system signals without accounting for the network constraints, (2). The resulting schedules are shown in Fig. 7(a) for Signal 1 and in Fig. 7(b) for Signal 2. As exemplified in Fig. 8 for the current at the main cable section, the obtained schedules result in a violation of the network limits. It can be observed that, even for Signal 2 where DR is allocated at times of low demand (if the devices are available at those times), the resulting currents can be up to ~600 A, which is twice the 300 A cable maximum capacity. Such overloading is a risk for network assets and power quality.

The outcomes from the DR scheduling, accounting now for network limits, are drawn in Fig. 9 and Fig. 10. In Fig. 9, the aggregated demand of all controllable devices is more evenly distributed, across the day, when compared to Fig. 7, with the results for both signals showing more flattened peaks; this can be associated with the limitation on the main cable current during such periods, which now, do not exceed the 300 A limit (see Fig. 10). These new DR schedules, different from those in Fig. 7, can be safely implemented (with appropriate corrections during real-time operation), highlighting the importance of considering the network constraints (2). Essentially, the schedules in Fig. 7 would overestimate the DR capacity that could be effectively achieved; note the expected DR peaks of ~330 kW in Fig. 7 vs. the ~200 kW in Fig. 9, i.e. network constraints limit the DR capability from Fig. 7 (based only on the controllable devices operational constraints) by up to ~40%.

From the obtained results, it is clear that the capacity of the residential sector to provide DR, at a specific time, can be limited by network constraints. This aspect is fundamental when assessing, at scale, the true DR capability that can be offered to the system. Furthermore, disregarding these constraints can jeopardize the electricity service quality and damage customer and network assets.

B. DR Real-Time Operation

1) Complying with day-ahead DR schedule

During operation, aggregators may need to modify the schedule from (1) due to differences between the real-time state of the network and the parameters defining the operational characteristics of the controllable devices (e.g. outside temperature) and the originally forecasted conditions. To do so, the problem (5), subject to (2)-(4), is solved at each control step.

Regarding the network constraints, the values of $Y^*_{forecast_{i,t}}$ for the definition of (9)-(10) are forecasted at each step based on new estimates from the DNO. An arbitrary value of 1×10^6 is selected for the penalization weights α_{P_t} (i.e., $\alpha_{P_t} \gg \sigma_{P_t}$) such that deviations from the DR schedule are as small as possible. In practice, the value of α_{P_t}could be set to be proportional to the impact of such deviations on system operation.

Fig. 11 shows the values obtained for P_{total_t} and for the consumed power of all controllable devices after operating the schedule in Fig. 9(b). While the power consumed by device type clearly deviates from the DR schedule, the total aggregated power closely follows the scheduled P_{total_t}. There is only a noticeable difference around 2 pm and 8 pm, due to the non-controllable demand component of the main cable section current being underestimated by the initial forecast around 1 pm (see Fig. 12). Such extra demand, observed during operation, had not taken place during the preceding days. For the aggregated consumed power by appliance type, differences between the schedule and operation are due to the latter having to adapt to the real-time network state (different of that originally forecasted). Compliance with the schedule and network constraints can result from multiple combinations of the power consumed by the devices at different houses, based on their sensitivities to the network variables.

2) Accuracy of Equations (9)-(10)

The daily profiles (from real-time operation of the schedule responding to Signal 2) of the actual values (obtained from power flow simulations in OpenDSS) and the results from (9)-(10) for the network variables considered in (2) are depicted in Fig. 13 and Fig. 14. In addition, Fig. 15 shows Equations (9)-(10) absolute error (i.e. difference from actual values) vs. total active power from DR. These values are for both Signal 1 and 2. Note that the sources of error in the LSE are limited to the pseudo-measurements (i.e. no error from measurements at the head of the feeder and for device consumed power).

For the voltages in Fig. 13, the results form (9)-(10) are very close to the actual values at times of large DR allocation, but less accurate when non-controllable demand is predominant. For the second case, differences are mainly due to the use of pseudo-measurements in the LSE. However, such situation is not a major problem as the distribution system should not, by design, experience problems due to non-controllable traditional demand [31]. Fig. 15(a) quantifies the above observations with errors of up to ~0.003 p.u. when P_{total} ~200 kW and errors of ~0.024 p.u. for P_{total} ~0 kW. While not occurring often, voltage limits can impose limitations to DR, as observed between 1 and 2 am for the phase *c* voltages in Fig. 13. During this period, DR is mainly dominated by SETS and EWH, which have been adopted by more phase *a* and phase *b* customers than by those in phase *c*. For instance, in Fig. 14, phases *a* and *b* are significantly more loaded between 1 and 2 am. A much higher loading in phases *a* and *b* can raise the voltage in phase *c* given that the phases are mutually coupled; this is a good example of how unbalanced systems can limit the hosting capacity of DR.

For the main cable section currents shown in Fig. 14, errors are almost negligible for most of the time as direct flow

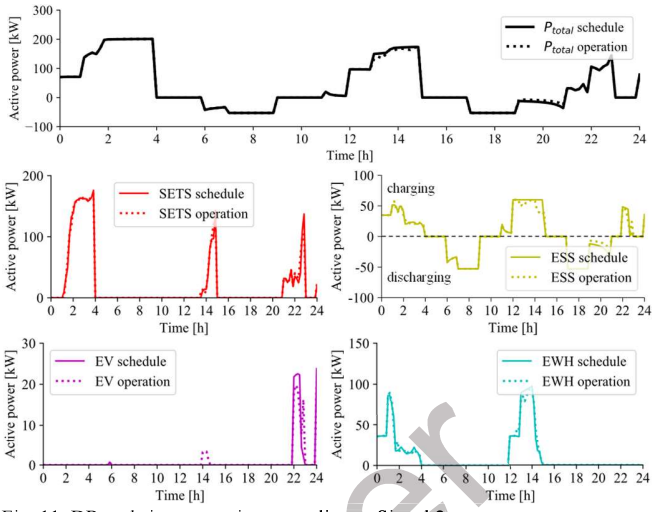

Fig. 11. DR real-time operation according to Signal 2

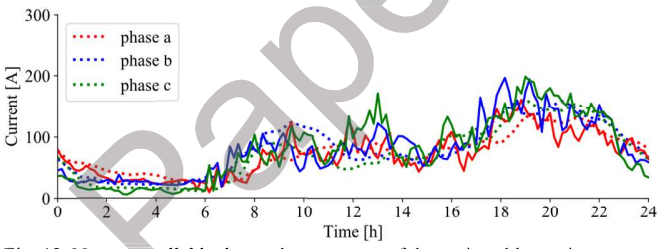

Fig. 12. Non-controllable demand component of the main cable section current flows. Actual values (solid lines) and forecasted values (dashed lines)

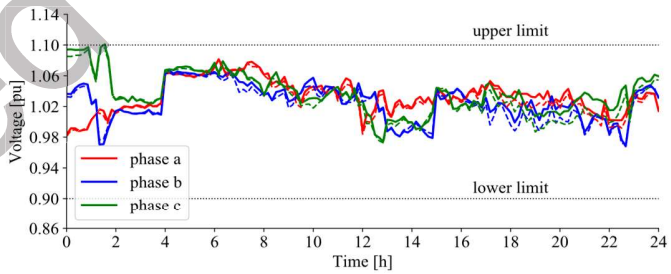

Fig. 13. End of the feeder voltages during DR operation (Signal 2). Actual values (solid lines) Aggregators expected values (dashed lines)

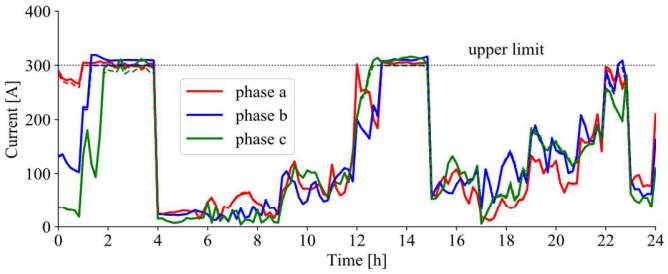

Fig. 14. Main cable section currents during DR operation (Signal 2). Actual values (solid lines) Aggregators expected values (dashed lines)

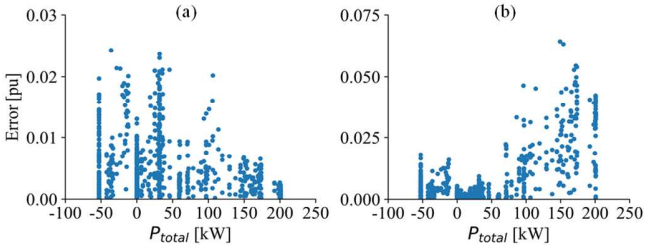

Fig. 15. Error from Equations (9)-(10) during real-time operation vs P_{total} for end of the feeder voltages (a) and head of the feeder current flows (b)

measurements are available at the transformer level. The only noticeable differences are at times of large DR allocation, when discrepancies can be attributed to the error from the sensitivities in (10). Fig. 15(b), quantifies the above observations with errors of up to 0.064 p.u. when P_{total} ~200 kW vs. errors of ~0.02 p.u. for P_{total} ~0 kW (using the cable rating as the base value). Note that, due to equations (9)-(10) being approximations, actual currents can exceed the cable rating in ~6.4%, something that can be conveniently overcome by operating with a small safety margin as discussed in Section VI.

VI. Discussion

A. Selecting Set of Constrained Network Variables

As discussed in Section III, aggregators receive estimations and sensitivities from the DNO of those network variables that are considered, by the latter, as key for safe network operation. These variables are constrained in (2). In order to avoid including unnecessary variables (e.g. voltages at nodes that are near the distribution transformer) and limit the computational complexity of the optimization problems, Section VI considers only those variables that have been defined as critical by previous DER integration studies [28], [42]. Nonetheless, different feeders may require, due to their topology and DER locations, to adopt a different set of variables. To define such a set, DNOs can use experience or perform studies such as those proposed in [22], where an impact assessment methodology certifies that network operational limits, considering that only a subset of the network variables is actively regulated, are respected under various operating ranges of its loads and DER.

B. Defining Safety Margins for the Network Statutory Limits

The expressions in (9) and (10), used by aggregators to formulate the network operational constraints in (2), will not perfectly characterize the actual value of the network variables, as shown in Fig. 13 to Fig. 15. For instance, the sensitivity coefficients in (9)-(10) are an approximation, and there will also be errors associated with the monitoring equipment used in the LSE. Consequently, safety margins will be required for the network operational limits to guarantee that the latter are not violated. The value of these margins should be defined by operators based on practical and/or empirical experience [22]. Note that safety margins are required regardless of which type of mathematical expression is used to characterize the network variables, due to errors associated with monitoring equipment, and network and DR modeling parameters.

C. Computational Times

The computational times taken by the LSE, sensitivity analysis and DR real-time operation problems will condition the real-time applicability of the methodology. Using an Intel Core i7-4790 CPU, the maximum values for these times were 10.3, 3.4 and 208.6 seconds, respectively. Note that for the sensitivity analysis, as no multi-period simulations were solved, low times were obtained due to parallel processing. In the case of the LSE, improved formulations could be used to reduce these times even further [25]. Note that the 3.4 minutes taken to solve the operational problem could be too high for actual operation. Nonetheless, this time is not representative of an actual implementation and corresponds to a worst-case scenario. First, as discussed in Section IV.B, aggregators are not expected to have direct control of DR devices (assumed in the test case) given that a centralized approach is expected to result in large computational times, as observed here. Instead, a decentralized multilevel approach for the aggregator/EMS interaction, which would reduce the complexity of the aggregator's problem, could take place. Under such an approach, EMS in-home controllers would solve their local DR problem (involving only those loads that are significant for DR provision) and iteratively interact with aggregators, similar to the approaches proposed in [11], [46]. Nonetheless, this paper's contribution relies upon the formulation of the network operational constraints (2); note that expressions (9)-(10) are independent of the type of aggregator/EMS interaction. Finally, the algorithms in Section III have not been optimized for speed and further improvements could be possible.

VII. Conclusions

This paper has introduced a methodology for the coordination of residential DR with the operational constraints of the local LV distribution network. The provision of DR, from aggregators to the system, is modeled as an optimization problem that accounts for the expected state of the network during DR scheduling and adapts to the actual state during real-time operation. Crucially, aggregators (with no direct access to network data) use representative data provided by the DNO to formulate a set of novel equations that characterize the magnitude of those network variables considered as key for safe network operation as a function of the DR allocation.

Using a representative feeder, the method is shown to be effective at dispatching DR without incurring in voltage and thermal problems. It is noted in this study that complying with network operational constraints can limit by up to 40% the allocation of DR at certain times. For other feeders, such limitation may be higher or lower depending on their topology, seasonality, and the level and type of DR. With the increasing adoption of DERs and the need for more system flexibility, methodologies such as that proposed here are expected to become more valuable in the near-term future.

Appendix

A. Controllable Electrical Devices Models

1) Smart electric thermal storage

SETS are electric space heaters that can draw power from the grid and store it in the form of heat [12] (typically by means of clay bricks or other ceramic materials), which can be released to regulate the dwelling's room temperature. In addition, SETS incorporate a boost element to provide extra heat, if needed. The operation of a set of S units for each single house can be described by:

$$P_t^{SETS} = \sum_s^S P_{t,s}^{SETS,ch} + P_{t,s}^{SETS,bst} \quad (12)$$

$$E_{t,s}^{SETS}\, N = E_{t-1,s}^{SETS}\,(N - 1 + \eta_s^{SETS}) + P_{t-1,s}^{SETS,ch} - P_{t-1,s}^{SETS,dis} \quad (13)$$

$$0 \le E_{t,s}^{SETS} \le E_{max}^{SETS} \quad (14)$$

$$0 \le P_{t,s}^{SETS,ch} \le P_{max}^{SETS,ch} \quad (15)$$

$$0 \le P_{t,s}^{SETS,bst} \le P_{max}^{SETS,bst} \quad (16)$$

$$0 \le P_{t,s}^{SETS,dis} \le P_{max}^{SETS,dis} \quad (17)$$

Equation (12) represents the aggregated demand of all SETS in the house. The energy stored by each device is described by (13) and constrained by (14). Equations (15)-(17) ensure that the charging, boost and discharging powers do not exceed their nominal ratings. The values used for the parameters in (12)-(17) are obtained from [12].

The dissipated heat, $Q_{t,s}^{SETS}$ in (18) maintains the indoor temperature, θ_t, within a desired range (19). The relationship between room temperature and $Q_{t,s}^{SETS}$ is defined by (20). Here, function g is obtained from the models proposed in [8]. Note that, for simplicity, internal disturbances are neglected in U_t.

$$Q_{t,s}^{SETS} = (1 - \eta_s^{SETS})\, E_{t,s}^{SETS} + P_{t,s}^{SETS,dis} + P_{t,s}^{SETS,bst} \quad (18)$$

$$\theta^{min} \le \theta_t \le \theta^{max} \quad (19)$$

$$\theta_{t+1} = \theta_t + g(\theta_t, Q_{t,s}^{SETS}, U_t, N) \quad (20)$$

2) Energy storage systems

ESSs can be modeled by equations (21)-(25). Assuming a single ESS unit per house, (21) defines the power consumed at the CPOC, with the charging and discharging power limited by (22)-(23). The state-of-charge (SOC) in (24) is constrained to be within the minimum and maximum limit in (25).

$$P_t^{ESS} = P_t^{ESS,ch} - P_t^{ESS,dis}\, \eta^{ESS,dis} \quad (21)$$

$$0 \le P_t^{ESS,ch} \le P_{max}^{ESS,ch} \quad (22)$$

$$0 \le P_t^{ESS,dis} \le P_{max}^{ESS,dis} \quad (23)$$

$$SOC_t^{ESS} = SOC_{t-1}^{ESS} + P_{t-1}^{ESS,ch}\, \eta^{ESS,ch}\, \frac{1}{N} - P_{t-1}^{ESS,dis}\, \frac{1}{N} \quad (24)$$

$$SOC^{ESS,min} \le SOC_t^{ESS} \le SOC^{ESS,max} \quad (25)$$

Integer variables are not necessary because of the losses, described by $\eta^{ESS,ch}$ and $\eta^{ESS,dis}$, avoid simultaneous charging and discharging, as the objective functions in the aggregator's optimization penalize unnecessary power consumption. The parameters in (21)-(25) are obtained from the model in [47].

3) Electric vehicles

EVs are modelled with equations (26)-(32). T^{EV} is the time at which each EV is expected to be connected to the network (26). During T^{EV}, the EV consumed power is limited by (27). Equation (28) describes the SOC, constrained to be within its limits by (29) and to reach its upper bound (i.e. fully charged) before a specified time by (30). Constraints (31)-(32) define the SOC for the initial time step, depending on whether the EV is connected or not to the grid; t_{init} is the first optimization step. EV characteristics are obtained from the trial described in [48].

$$T^{EV} = \left[T_{EV}^{a}, T_{EV}^{f}\right] \cap T \quad (26)$$

$$0 \le P_t^{EV} \le P_t^{EV,max} \quad \forall t \in T^{EV} \quad (27)$$

$$SOC_t^{EV} = SOC_{t-1}^{EV} + P_{t-1}^{EV}\, \eta^{EV}\, \frac{1}{N} \quad \forall t \in T^{EV} \quad (28)$$

$$SOC^{EV,min} \le SOC_t^{EV} \le SOC^{EV,max} \quad (29)$$

$$SOC_t^{EV} = SOC^{EV,max} \text{ if } t = T_{EV}^{f} \text{ and } T_{EV}^{f} \in T^{EV} \quad (30)$$

$$SOC_t^{EV} = SOC^{EV,start} \text{ if } t = T_{EV}^{a} \text{ and } T_{EV}^{a} \in T^{EV} \quad (31)$$

$$SOC_t^{EV} = SOC^{EV,init} \text{ if } t = t_{init} \text{ and } T_{EV}^{a} \notin T^{EV} \quad (32)$$

4) Electric water heaters

For EWHs, customer comfort is characterized as the need to consume a certain volume of energy before a specific time. Using a set of hot water demand profiles generated with the statistical demand model from [8], two hot water demand peaks are identified for each house (morning and evening), together with the required energy volume. Using these values, EWH operation is described by:

$$0 \le P_t^{EWH} \le P_{max}^{EWH} \quad \forall t \ni t \le T_{evening}^{pk} \quad (33)$$

if $T_{morning}^{pk} \in T$:

$$E_{morning}\, N = E_{morning}^{init} + \sum_{t}^{[1,\ldots,T_{morning}^{pk}]} P_t^{EWH} \quad (34)$$

$$E_{evening}\, N = \sum_{t}^{[T_{morning}^{pk}+1,\ldots,T_{evening}^{pk}]} P_t^{EWH} \quad (35)$$

else, if $T_{morning}^{pk} \notin T$ and $T_{evening}^{pk} \in T$:

$$E_{evening}\, N = E_{evening}^{init} + \sum_{t}^{[1,\ldots,T_{evening}^{pk}]} P_t^{EWH} \quad (36)$$

where (33) limits EWH power to its rating and constraints (34)-(36) ensure customer satisfaction. Note that $E_{morning}^{init}|E_{evening}^{init}$ are the energy, by peak, that has been consumed in the previous control steps. The value of P_{max}^{EWH} is obtained from [35].

REFERENCES

[1] E. McKenna, P. Grünewald, and M. Thomson, "Going with the wind: Temporal characteristics of potential wind curtailment in Ireland in 2020 and opportunities for demand response," *IET Renew. Power Gener.*, vol. 9, no. 1, pp. 66–77, 2015, doi: 10.1049/iet-rpg.2013.0320.

[2] B. Dupont, K. Dietrich, C. De Jonghe, A. Ramos, and R. Belmans, "Impact of residential demand response on power system operation: A Belgian case study," *Appl. Energy*, vol. 122, pp. 1–10, 2014, doi: 10.1016/j.apenergy.2014.02.022.

[3] Low Carbon Innovation Coordination Group, "Carbon Innovation Coordination Group Technology Innovation Needs Assessment (TINA) Marine Energy Summary Report," 2012.

[4] J. Quirós-Tortós, L. (Nando) Ochoa, and T. Butler, "How Electric Vehicles and the Grid Work Together," *IEEE Power and Energy Magazine*, no. October 2018, pp. 64–76, 2018.

[5] S. Burger, J. P. Chaves-Ávila, C. Batlle, and I. J. Pérez-Arriaga, "A review of the value of aggregators in electricity systems," *Renewable and Sustainable Energy Reviews*, vol. 77. pp. 395–405, 2017, doi: 10.1016/j.rser.2017.04.014.

[6] P. Siano, "Demand response and smart grids - A survey," *Renew. Sustain. Energy Rev.*, vol. 30, pp. 461–478, 2014, doi: 10.1016/j.rser.2013.10.022.

[7] P. Grünewald, E. McKenna, and M. Thomson, "Keep it simple: Time-of-use tariffs in high-wind scenarios," *IET Renew. Power Gener.*, vol. 9, no. 2, pp. 176–183, 2015, doi: 10.1049/iet-rpg.2014.0031.

[8] E. McKenna and M. Thomson, "High-resolution stochastic integrated thermal-electrical domestic demand model," *Appl. Energy*, vol. 165, pp. 445–461, 2016, doi: 10.1016/j.apenergy.2015.12.089.

[9] K. Dietrich, J. M. Latorre, L. Olmos, and A. Ramos, "Demand response in an isolated system with high wind integration," *IEEE Trans. Power Syst.*, vol. 27, no. 1, pp. 20–29, 2012, doi: 10.1109/TPWRS.2011.2159252.

[10] J. Medina, N. Muller, and I. Roytelman, "Demand response and distribution grid operations: Opportunities and challenges," *IEEE Trans. Smart Grid*, vol. 1, no. 2, pp. 193–198, 2010, doi: 10.1109/TSG.2010.2050156.

[11] W. Shi, N. Li, X. Xie, C. C. Chu, and R. Gadh, "Optimal residential demand response in distribution networks," *IEEE J. Sel. Areas Commun.*, vol. 32, no. 7, pp. 1441–1450, 2014, doi: 10.1109/JSAC.2014.2332131.

[12] M. Bakhtvar, C. A. Cabrera, G. Buttitta, O. Neu, and A. Keane, "A study of operation strategy of small scale heat storage devices in residential distribution feeders," in *2017 IEEE PES Innovative Smart Grid*

Technologies Conference Europe, ISGT-Europe 2017 - Proceedings, 2017, vol. 2018-Janua, pp. 1–6, doi: 10.1109/ISGTEurope.2017.8260254.

[13] E. Vrettos and G. Andersson, "Combined load frequency control and active distribution network management with thermostatically controlled loads," in *2013 IEEE International Conference on Smart Grid Communications, SmartGridComm 2013*, 2013, pp. 247–252, doi: 10.1109/SmartGridComm.2013.6687965.

[14] E. D. Anese, S. S. Guggilam, A. Simonetto, Y. C. Chen, and S. V. Dhople, "Optimal Regulation of Virtual Power Plants," *IEEE Trans. Power Syst.*, vol. 33, no. 2, pp. 1868–1881, 2018, doi: 10.1109/TPWRS.2017.2741920.

[15] A. Hassan, R. Mieth, M. Chertkov, D. Deka, and Y. Dvorkin, "Optimal Load Ensemble Control in Chance-Constrained Optimal Power Flow," *IEEE Trans. Smart Grid*, 2018, doi: 10.1109/TSG.2018.2878757.

[16] L. Gkatzikis, I. Koutsopoulos, and T. Salonidis, "The role of aggregators in smart grid demand response markets," *IEEE J. Sel. Areas Commun.*, vol. 31, no. 7, pp. 1247–1257, 2013, doi: 10.1109/JSAC.2013.130708.

[17] K. Samarakoon, J. Ekanayake, and N. Jenkins, "Reporting available demand response," *IEEE Trans. Smart Grid*, vol. 4, no. 4, pp. 1842–1851, 2013, doi: 10.1109/TSG.2013.2258045.

[18] Eurelectric, "CEER public consultation 'The Future role of DSOs,'" 2015.

[19] S. C. Ross, N. Ozay, and J. L. Mathieu, "Coordination between an aggregator and distribution operator to achieve network-aware load control," in *2019 IEEE Milan PowerTech, PowerTech 2019*, 2019, doi: 10.1109/PTC.2019.8810635.

[20] N. G. Paterakis, O. Erdinç, A. G. Bakirtzis, and J. P. S. Catalão, "Optimal household appliances scheduling under day-ahead pricing and load-shaping demand response strategies," *IEEE Trans. Ind. Informatics*, vol. 11, no. 6, pp. 1509–1519, 2015, doi: 10.1109/TII.2015.2438534.

[21] A. Abur and A. G. Exposito, *Power System State Estimation: Theory and Implementation*. 2004.

[22] D. Molzahn and L. A. Roald, "Grid-Aware versus Grid-Agnostic Distribution System Control: A Method for Certifying Engineering Constraint Satisfaction," in *Proceedings of the 52nd Hawaii International Conference on System Sciences*, 2019, doi: 10.24251/hicss.2019.417.

[23] R. Singh, B. C. Pal, and R. A. Jabr, "Distribution system state estimation through Gaussian mixture model of the load as pseudo-measurement," *IET Gener. Transm. Distrib.*, vol. 4, no. 1, pp. 50–59, 2010, doi: 10.1049/iet-gtd.2009.0167.

[24] P. A. N. Garcia, J. L. R. Pereira, S. Carneiro, and V. M. Da Costa, "Three-phase power flow calculations using the current injection method," *IEEE Trans. Power Syst.*, vol. 15, no. 2, pp. 508–514, 2000, doi: 10.1109/59.867133.

[25] M. C. De Almeida and L. F. Ochoa, "An Improved Three-Phase AMB Distribution System State Estimator," *IEEE Trans. Power Syst.*, vol. 32, no. 2, pp. 1463–1473, 2017, doi: 10.1109/TPWRS.2016.2590499.

[26] G. Valverde and T. Van Cutsem, "Model predictive control of voltages in active distribution networks," *IEEE Trans. Smart Grid*, vol. 4, no. 4, pp. 2152–2161, 2013, doi: 10.1109/TSG.2013.2246199.

[27] Z. Zhang, L. F. Ochoa, and G. Valverde, "A Novel Voltage Sensitivity Approach for the Decentralized Control of DG Plants," *IEEE Transactions on Power Systems*, vol. 33, no. 2, pp. 1566–1576, 2018.

[28] V. Rigoni and A. Keane, "Estimation of voltage sensitivities in low voltage feeders with photovoltaics," in *Proceedings - 2018 IEEE PES Innovative Smart Grid Technologies Conference Europe, ISGT-Europe 2018*, 2018, doi: 10.1109/ISGTEurope.2018.8571580.

[29] F. Tamp and P. Ciufo, "A sensitivity analysis toolkit for the simplification of MV distribution network voltage management," *IEEE Trans. Smart Grid*, vol. 5, no. 2, pp. 559–568, 2014, doi: 10.1109/TSG.2014.2300146.

[30] S. C. Chapra and R. P. Canale, *Numerical methods for engineers*, vol. 33, no. 3. 1991.

[31] A. Navarro-Espinosa and L. F. Ochoa, "Probabilistic Impact Assessment of Low Carbon Technologies in LV Distribution Systems," *IEEE Transactions on Power Systems*, vol. 31, no. 3, pp. 2192–2203, 2016.

[32] EirGrid and SONI, "DS3 System Services," 2017.

[33] OMIE, "Market Results," *Market Results*, 2013. [Online]. Available: http://www.omel.es/files/flash/ResultadosMercado.swf.

[34] EirGrid, "EirGrid Group plc - Smart Grid Dashboard," *EirGrid Group*, 2017. [Online]. Available: http://smartgriddashboard.eirgrid.com/#all/wind.

[35] K. McKenna and A. Keane, "Residential Load Modeling of Price-Based Demand Response for Network Impact Studies," *IEEE Transactions on Smart Grid*, vol. 7, no. 5. pp. 2285–2294, 2016, doi: 10.1109/TSG.2015.2437451.

[36] R. Henriquez, G. Wenzel, D. E. Olivares, and M. Negrete-Pincetic, "Participation of demand response aggregators in electricity markets: Optimal portfolio management," *IEEE Trans. Smart Grid*, vol. 9, no. 5, pp. 4861–4871, 2018, doi: 10.1109/TSG.2017.2673783.

[37] ENWL, "LV Network Models (Dataset)," *Low Voltage Network Solutions*, 2014.

[38] V. Rigoni, L. F. Ochoa, G. Chicco, A. Navarro-Espinosa, and T. Gozel, "Representative residential LV feeders: A case study for the North West of England," *IEEE Trans. Power Syst.*, vol. 31, no. 1, pp. 348–360, 2016, doi: 10.1109/TPWRS.2015.2403252.

[39] Y. Li and P. J. Wolfs, "Taxonomic description for western Australian distribution medium-voltage and low-voltage feeders," *IET Gener. Transm. Distrib.*, vol. 8, no. 1, pp. 104–113, 2014, doi: 10.1049/iet-gtd.2013.0005.

[40] M. Hijhuis, M. Gibescu, and S. Cobben, "Clustering of Low Voltage Feeders from a Network Planning Perspective," in *23nd International Conference on Electricity Distribution (CIRED)*, 2015, pp. 1–5.

[41] T. S. Chu, "Polarization Properties of Offset Dual-Reflector Antennas," *IEEE Transactions on Antennas and Propagation*, 1991. .

[42] J. Quirós-Tortós, L. F. Ochoa, S. W. Alnaser, and T. Butler, "Control of EV Charging Points for Thermal and Voltage Management of LV Networks," *IEEE Trans. Power Syst.*, vol. 31, no. 4, pp. 3028–3039, 2016, doi: 10.1109/TPWRS.2015.2468062.

[43] EPRI, "OpenDSS - Open Distribution System Simulator," *Smartgrid.Epri.Com*. 2014.

[44] W. E. Hart, C. Laird, J.-P. Watson, and D. L. Woodruff, "Pyomo – Optimization Modeling in Python," *Adv. Model. Agric. Syst.*, vol. 67, pp. 13–28, 2012, doi: 10.1007/978-1-4614-3226-5.

[45] R. H. Byrd, J. Nocedal, and R. A. Waltz, "Knitro: An Integrated Package for Nonlinear Optimization," *Energy*, vol. 83, pp. 35–59, 2006, doi: 10.1007/0-387-30065-1_4.

[46] M. Rastegar, M. Fotuhi-Firuzabad, and M. Moeini-Aghtai, "Developing a two-level framework for residential energy management," *IEEE Trans. Smart Grid*, 2018, doi: 10.1109/TSG.2016.2598754.

[47] A. T. Procopiou, K. Petrou, L. F. Ochoa, T. Langstaff, and J. Theunissen, "Adaptive decentralized control of residential storage in pv-rich mv-lv networks," *IEEE Trans. Power Syst.*, vol. 34, no. 3, pp. 2378–2389, 2019, doi: 10.1109/TPWRS.2018.2889843.

[48] P. Richardson, D. Flynn, and A. Keane, "Impact assessment of varying penetrations of electric vehicles on low voltage distribution systems," *IEEE PES Gen. Meet. PES 2010*, pp. 1–6, 2010, doi: 10.1109/PES.2010.5589940.